

2-13-2019

Designing Morphotropic Phase Composition in BiFeO₃

Andreas Herklotz

Oak Ridge National Laboratory

Stefania F. Rus

National Institute for Research and Development in Electrochemistry and Condensed Matter

Nina Balke

Oak Ridge National Laboratory

Christopher Rouleau

Oak Ridge National Laboratory

Er-Jia Guo

Oak Ridge National Laboratory

See next page for additional authors

Follow this and additional works at: https://lib.dr.iastate.edu/ameslab_manuscripts



Part of the [Condensed Matter Physics Commons](#), and the [Nanoscience and Nanotechnology Commons](#)

Recommended Citation

Herklotz, Andreas; Rus, Stefania F.; Balke, Nina; Rouleau, Christopher; Guo, Er-Jia; Huon, Amanda; KC, Santosh; Roth, Robert; Yang, Xu; Vaswani, Chirag; Wang, Jigang; Orth, Peter P.; Scheurer, Mathias S.; and Ward, Thomas Z., "Designing Morphotropic Phase Composition in BiFeO₃" (2019). *Ames Laboratory Accepted Manuscripts*. 546.

https://lib.dr.iastate.edu/ameslab_manuscripts/546

This Article is brought to you for free and open access by the Ames Laboratory at Iowa State University Digital Repository. It has been accepted for inclusion in Ames Laboratory Accepted Manuscripts by an authorized administrator of Iowa State University Digital Repository. For more information, please contact digirep@iastate.edu.

Designing Morphotropic Phase Composition in BiFeO₃

Abstract

In classical morphotropic piezoelectric materials, rhombohedral and tetragonal phase variants can energetically compete to form a mixed phase regime with improved functional properties. While the discovery of morphotropic-like phases in multiferroic BiFeO₃ films has broadened this definition, accessing these phase spaces is still typically accomplished through isovalent substitution or heteroepitaxial strain which do not allow for continuous modification of phase composition postsynthesis. Here, we show that it is possible to use low-energy helium implantation to tailor morphotropic phases of epitaxial BiFeO₃ films postsynthesis in a continuous and iterative manner. Applying this strain doping approach to morphotropic films creates a new phase space based on internal and external lattice stress that can be seen as an analogue to temperature–composition phase diagrams of classical morphotropic ferroelectric systems.

Keywords

Morphotropic phases, strain, ferroelectrics, implantation, metastability

Disciplines

Condensed Matter Physics | Nanoscience and Nanotechnology

Authors

Andreas Herklotz, Stefania F. Rus, Nina Balke, Christopher Rouleau, Er-Jia Guo, Amanda Huon, Santosh KC, Robert Roth, Xu Yang, Chirag Vaswani, Jigang Wang, Peter P. Orth, Mathias S. Scheurer, and Thomas Z. Ward

Designing Morphotropic Phase Composition in BiFeO₃

Andreas Herklotz^{1,2}, Stefania F. Rus³, Nina Balke Wisinger⁴, Christopher Rouleau⁴, Er-Jia Guo⁵, Amanda Huon^{1,6}, Santosh KC¹, Robert Roth,² Xu Yang⁷, Chirag Vaswani⁷, Jigang Wang⁷, Peter P. Orth⁷, Mathias S. Scheurer⁸ and Thomas Z. Ward^{1,*}

¹ Materials Science and Technology Division, Oak Ridge National Laboratory, Oak Ridge, TN, 37831, USA

² Institute for Physics, Martin Luther University of Halle-Wittenberg, Halle, Germany

³ Renewable Energies Laboratory Photovoltaics, National Institute for Research and Development in Electrochemistry and Condensed Matter, Timisoara, 300713, Romania

⁴ Center for Nanophase Materials Sciences, Oak Ridge National Laboratory, Oak Ridge, TN, 37831, USA

⁵ Neutron Scattering Division, Oak Ridge National Laboratory, Oak Ridge, TN, 37831, USA

⁶ Department of Materials Science and Engineering, Drexel University, Philadelphia, PA, 19104, USA

⁷ Department of Physics and Astronomy and Ames Laboratory-U.S. DOE, Iowa State University, Ames, IA, 50011, USA

⁸ Department of Physics, Harvard University, Cambridge, MA, 02138, USA

* wardtz@ornl.gov

Abstract:

In classical morphotropic piezoelectric materials, rhombohedral and tetragonal phase variants can energetically compete to form a mixed phase regime with improved functional properties. While the discovery of morphotropic-like phases in multiferroic BiFeO₃ films has broadened this definition, accessing these phase spaces is still typically accomplished through isovalent substitution or heteroepitaxial strain which do not allow for continuous modification of phase composition post-synthesis. Here, we show that it is possible to use low-energy helium implantation to tailor morphotropic phases of epitaxial BiFeO₃ films post-synthesis in a continuous and iterative manner. Applying this strain doping approach to morphotropic films creates a new phase space based on internal and external lattice stress that can be seen as an analogue to temperature – composition phase diagrams of classical morphotropic ferroelectric systems.

Keywords: Morphotropic phases, strain, ferroelectrics, implantation, metastability

Main Text:

Structural phase transitions are quite common in complex oxides such as perovskites, where energetic differences between configurations of oxygen octahedral arrangements or polar distortions are generally subtle. As such, small external perturbations of the crystal lattice have the potential to shift the energy balance of competing crystal phases and drive transitions to states with unknown functionalities. As one of the few room temperature multiferroics, BiFeO₃ (BFO) is an excellent example.¹⁻³ Compressive in-plane strain in

epitaxial BFO films can induce a transition from a bulk-like rhombohedral polymorph (R) to a tetragonal variant (T) with an extremely high c/a axis ratio and vastly different physical properties. This observation is particularly intriguing since it resembles a strain-driven morphotropic phase transition of a single material in analogy to the compositionally controlled classical morphotropic phase boundary between two materials with rhombohedral and tetragonal structure. Furthermore, just as the monoclinic phases in many classical morphotropic systems, such as $\text{PbZr}_x\text{Ti}_{1-x}\text{O}_3$, the strain-driven morphotropic phase boundary (MPB) in BFO involves an additional “S” polymorph that bridges the transition between the R-like and T-like state.^{4,5} These lower-symmetry phases are of crucial importance to the extraordinarily high electromechanical response of morphotropic systems near the MPB.⁶⁻⁹ It is now well established that lattice strain induced by chemical pressure is the main driving force of compositionally driven MPBs in classical ferroelectrics.¹⁰ This finding implies that tailoring the competition between crystal phases by strain rather than composition might serve as a general avenue to extend our understanding of morphotropic systems and pave the way to new applications.^{10,11}

There are severe limitations to the execution of this approach using traditional strain engineering methods. Hetero-epitaxy approaches only allow discrete strain regimes dictated by available substrates and do not permit the continuous strain tunability needed to fully explore phase spaces around MPB's. Further, epitaxy and isovalent substitution methods do not allow the manipulation of local strain states nor do they permit the application of iterative strain accumulation post-growth. Ion implantation is a highly tunable process that can be applied post-synthesis to virtually any thin film system. For example, irradiation of ferroelectric films with high-energy noble gas ions has successively been applied to tailor switching kinetics via the selective introduction of defects.^{12,13} However, control of competing morphotropic phases has not been demonstrated so far. Focusing on low-energy He ion

implantation we have recently shown as an effective means of manipulating strain states of epitaxial oxide thin films.^{14,15} We show that strain doping with ion irradiation can be used to bypass these limitations and provide access to large regions of morphotropic phase spaces. We demonstrate that this strain doping approach can be used to modify the competition of morphotropic BFO phases leading to a complete transition from R-like to T-like polymorph's. In addition, strain doping can be used to expose previously inaccessible boundaries in BFO's structural phase space. The findings show that ion implantation provides a means to more fully interrogate morphotropic systems, which may allow access to previously hidden functionalities while offering the versatility to exploit these properties through a simple *ex situ* post-growth process.

By growing epitaxial BFO films on a range of progressively smaller lattice matched substrates, it is possible to use as-grown in-plane strain states to generate discrete phase compositions at different locations of the BFO morphotropic phase space.¹ In this work, epitaxial BFO films are grown on three different (001) oriented substrates, SrTiO₃ (STO), (LaAlO₃)_{0.3}(Sr₂TaAlO₆)_{0.7} (LSAT) and LaAlO₃ (LAO) to give varied starting locations in the morphotropic phase space. X-ray diffraction confirms that all films are grown coherently with their substrates, with an increasing compressive in-plane strain of -1.4% for STO, -2.5% for LSAT, and -4.6% for LAO. The films' structures are in perfect agreement with previous reports on epitaxial BFO films—with the films on STO and LSAT growing in R-like states^{16,17} and the film on LAO growing in a T-like state.¹⁸

Helium ion implantation is used iteratively to strain dope each of the three films across a range of expansions (see Supporting Information). **Figure 1a** shows θ - 2θ XRD scans around the 002_{pc} peak of BFO with successively increasing He doses. A continuous *c*-axis lattice expansion is observed in each of the films by a shift to lower peak angles with increasing ion dose. However, a closer look at the lattice parameters as a function of the He dose reveals

important differences (**Fig. 1b**). While the film on STO shows a linear expansion with increasing He dose, the expansion of the films on LAO and LSAT is non-linear. This non-linear expansion is a hallmark of crossing morphotropic phase boundaries. The film on LSAT undergoes a complete R→T transformation to a supertetragonal state ($c/a = 1.21$). This transition demonstrates the ability to control the morphotropic BFO phases in a manner impossible using heteroepitaxy or isovalent substitution. While these traditional methods require the phase composition to be set during the growth process, the strain doping approach allows for precise and iterative post-synthesis manipulation of phases, thereby opening the door to exploring previously inaccessible regions near phase boundaries where functionally relevant metastabilities can be expected.

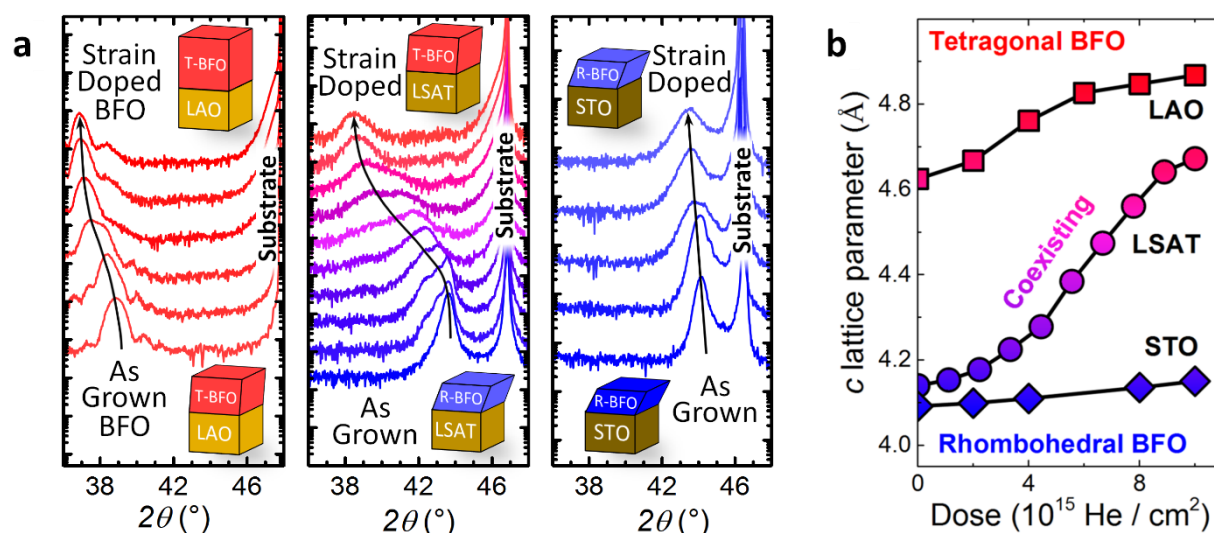


Figure 1. Structural changes of BFO thin films upon He ion irradiation. (a) θ - 2θ scans around the 002_{pc} peaks of BFO thin films on LAO, LSAT and STO substrates under different helium dosage. The black arrows illustrate the shifts of the XRD film peak with increasing doping. (b) The out-of-plane lattice constant c as a function of helium dose. A nonlinear behavior due to crystal phase transitions is clearly visible for the film on LSAT and LAO.

One means to make transient observations of morphotropic phase space is by using temperature dependent studies, which allow thermal expansion to drive phase composition transitions.^{19,20} As-grown BFO films on LAO typically show a rich pattern of mixed phase nanodomains embedded in a matrix of a macroscopically tetragonal phase.²¹ These nanodomains are known to consist of stripes of highly distorted variants of T-like BFO (T^{tilt})

and S-BFO (S^{tilt}) that are energetically favorable to promote strain relaxation towards the significantly less distorted R-like BFO.^{20,22} With increasing temperature, the nanodomains progressively disappear as the BFO film transitions to a single-domain T-like state.²⁰ **Figure 2** demonstrates how strain doping allows for the stabilization of all of the morphotropic phase compositions previously only accessible through transient thermal expansions—allowing one to progress from the mixed phase polymorph dominated as-grown state to a pure tetragonal state at room temperature.

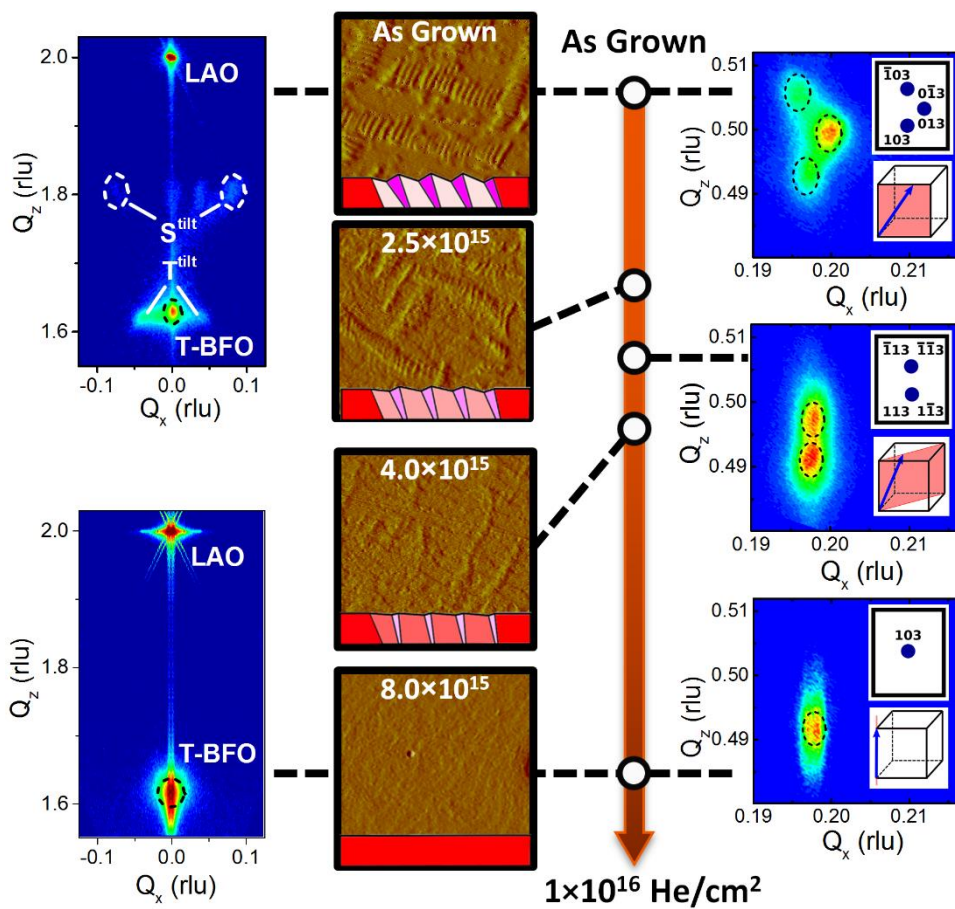


Figure 2. Effect of strain doping on phase competition and crystal structure of BFO/LAO. **(Left)** RSMs around the 002_{pc} reflections of as-grown undosed (top) and highly dosed (8×10^{15} He/cm², bottom) BFO films, respectively. **(Center)** Topographic AFM images of 2.5 μm on a side recorded after subsequent dosing confirm the disappearance of mixed phase nanodomains and the transformation into a uniform single-domain film. The insets illustrate schematically the transition of S to T polymorphs under strain doping resulting in a decrease of the tilting angles and a weakening of the topographic contrast between strip-like nanodomains. **(Right)** RSM space maps around the 103_{pc} reflections of as-grown, intermediate (3.5×10^{15} He/cm²) and highly dosed (8×10^{15} He/cm²) BFO films. The change from a three XRD peak pattern to a two peak and one peak pattern shows the crystal structure transformation of T-like BFO from a monoclinic M_C -type to monoclinic M_A -type and tetragonal T -type structure, respectively.

Atomic force microscopy (AFM) of the as-grown BFO film on LAO shows a clear pattern of nanodomains. Additionally, off-specular peaks in reciprocal space maps (RSM) around the 002_{pc} reflection of BFO confirm the presence of the expected tilted phases. An RSM around the 103_{pc} reflection of the as-grown film shows splitting into three subpeaks indicating that the lattice of the untilted T-BFO is accurately described by a M_C -type monoclinic distortion to the tetragonal structure. With increasing He dose, the height contrast of the mixed phase nanodomains as seen in AFM images is continuously decreasing. Simultaneously, the 103_{pc} XRD reflections of an intermediate dosed BFO film change to a pattern of two vertically aligned peaks. This indicates that He implantation shifts the balance between tilted S and T phases, while the macroscopically untilted phase undergoes a phase transition towards a $T(M_A)$ -type monoclinic distortion. Increasing the He dose even further leads to a complete disappearance of nanodomains -recognized by the homogeneous atomically flat topography in AFM and by the absence of any tilted phases in the RSM around the 002_{pc} reflection. The RSM around the 103_{pc} reflection shows a single peak, meaning that the highly dosed film is a uniform single-domain film of tetragonal $T(T)$ -like phase. We conclude that BFO films undergo a $M_C \rightarrow M_A \rightarrow T$ sequence of structural phase transitions upon He implantation. The fact that this sequence is identical to that observed with transient thermal expansion may have interesting implications for fundamental and applied studies that were previously impeded by the need to work at elevated temperatures.

Imposing different substrate-induced in-plane strain modifies the phase balance of competing polymorphs in as-grown BFO films. Applying strain doping to these independent starting points permits exploration of previously inaccessible phase spaces. While BFO grown on LAO is well known to possess mixed phases, films grown on less compressive substrates, such as LSAT, are typically in a pure R-like state. **Figure 3** summarizes the effects of

iterative strain doping on BFO grown on LSAT. Upon strain doping, the R phase directly transitions to the T phase. This allows for the selective design of the R/T phase ratio in a single crystal film (Fig. 3a-b). The S phase is not present at any doping level. This observation reveals a fundamentally important point; the S phase is not required as intermediary phase when transitioning between R and T phases as has been previously suggested.²⁰

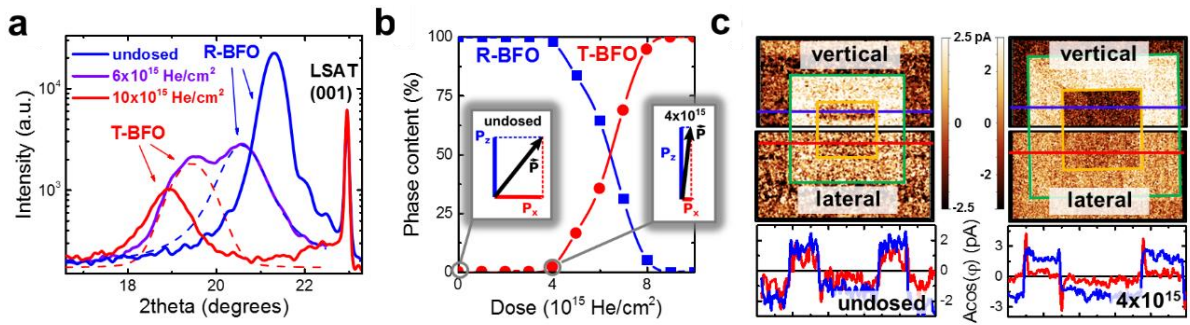


Figure 3. Effect of strain doping on BFO/LSAT. (a) θ - 2θ scans around the 001_{pc} peaks of a BFO film in an as-grown undosed, intermediate, and highly dosed state. Fitting to the data in the intermediate state demonstrates that the film shows two XRD peaks that can be ascribed to the coexistence of R and T-like BFO. (b) Phase content of R and T-like BFO as determined by the area of the XRD peaks as function of He dose. (c) vertical and lateral PFM data on an undosed BFO film (left) and a film dosed with 4×10^{15} He/cm² (right). The images were recorded after writing a square of $4 \times 4 \mu\text{m}$ under negative bias (green box; -3V for undosed and -8V for dosed film) followed by writing the inner square under a positive bias (orange; 3/8V). The undosed film shows a strong contrast in both vertical and the lateral piezoresponse, clearly indicating a significant in-plane component of the ferroelectric polarization as schematically illustrated in the inset. Line scans are shown to demonstrate the contrast between positively and negatively switched regions in both images. The dosed film exhibits a clear contrast in the vertical response, while the lateral contrast has almost vanished. This observation suggests that the polarization has rotated almost entirely towards the film normal.

The control of mixed BFO phases and stabilization of single-domain T-BFO by strain is intimately coupled to the mechanism of polarization rotation well known from standard morphotropic ferroelectrics.²⁰ The $R \rightarrow M_C \rightarrow M_A \rightarrow T$ phase sequence of BFO under compressive in-plane strain^{23,24} displays a typical rotation path that is also found in other systems such as PZT and PMN-PT when a rotation of the polarization vector from in-plane to out-of-plane is triggered upon application of an electric field or changes of temperature.^{8,20,25,26} The direct $R \rightarrow T$ transformation found under strain doping in films grown on LSAT represents a transition that requires a group-subgroup symmetry relationship

between the R- and T polymorphs of BFO and appears to be at odds with the idea of a continuous polarization rotation. However, piezoresponse force microscopy (PFM) on $\text{La}_{0.7}\text{Sr}_{0.3}\text{MnO}_3$ (LSMO) buffered BFO/LSMO/LSAT films demonstrates that upon strain doping the ferroelectric polarization is already rotating almost entirely into the film normal prior to the actual phase transition (**Fig 3c**). The measurement of macroscopic polarization loops that would support the observation of polarization rotation was unfortunately prevented by high leakage currents typical for thin BFO films. By conducting second-harmonic generation (SHG) measurements on the BFO/LSAT system (see Supporting Information for details), we can identify important information on the type of order that is allowed by symmetry. We find that for all doses the electronic order is consistent with a point group symmetry of C_{2v} (or C_4). This indicates that the R \rightarrow T-like transition does not involve a change of internal symmetry, corroborating the model of polarization rotation. The continuous control of polarization orientation through strain doping represents a degree of functionality that is not accessible by common approaches.

By combining epitaxial strain and strain doping, we are effectively creating a new phase space, as schematically illustrated in **Figure 4**. This phase space based on internal – external lattice stress displays strong analogies to the temperature – composition phase diagrams of standard morphotropic ferroelectric systems (see inset). While the epitaxial in-plane strain of films grown on LAO drives BFO towards a mixed phase state, similar to monoclinic regions at morphotropic phase boundaries of lead-based ferroelectrics, strain doping shifts the phase balance to a purely tetragonal state. The lower in-plane strain of films on LSAT appears to shift the system to a state that is similar to the region near the triple point in the classical phase diagram that display direct transitions between R and T phases over a narrow composition range.¹⁹ DFT predictions on BFO have shown that R and T polymorphs are energetically degenerate under moderate compressive in-plane strain, thus the observations of

direct R→T transitions are not so surprising.^{22,27} In particular, the free energy landscape is extremely flat in an out-of-plane-only lattice expansion scenario²⁸, which means that a direct transition is thermodynamically allowed.²⁹ Smaller epitaxial in-plane strain, as for films grown on STO, increases the energy difference and favors the stabilization of R-like BFO. Consequently, no phase transitions are observed under strain doping.

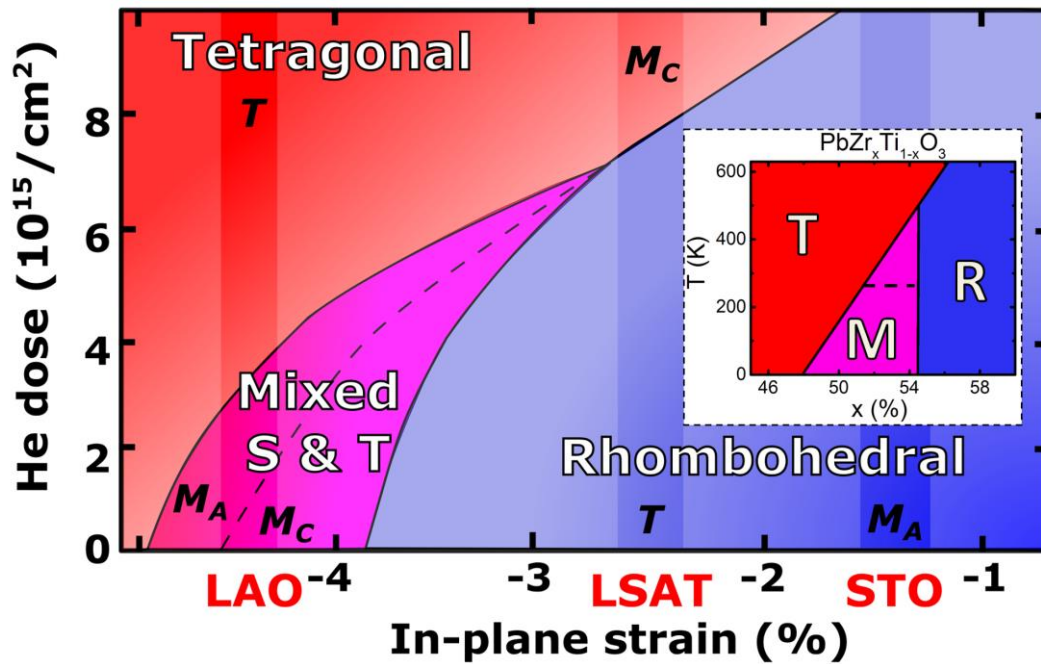


Figure 4. Schematic phase diagram based on the structural characterization of strain-doped BFO films. The inset shows the temperature - composition phase diagram of the classical morphotropic $\text{PbZr}_x\text{Ti}_{1-x}\text{O}_3$ system for comparison.¹⁹

Helium ion implantation into epitaxial BFO films is an efficient way to manipulate morphotropic phases of epitaxial thin films. Although substitutional doping is applied regularly to tailor ferroelectrics,^{30–33} strain doping differs from these approaches and comes with significant advantages. The inclusion of noble He into a film’s lattice introduces internal stress but does not create major changes to bond configurations as compared to standard doping with ions. Most importantly, ion implantation is a highly tunable process that can be employed post-synthesis and can be combined with lithography to create novel functionalities.³⁴ In the case of BFO films for example, one may think of creating regular patterns of T-like domains in an R-like matrix that could be used to fabricate entirely new

devices that harness the vastly different electrical, (thermo)mechanical, or optical properties of T and R phases. The findings described should be universally applicable to virtually any thin film system where competing crystal phases are used to drive functionality. This pool of systems includes any type of ferroic material where strain doping affects order parameters, but could be extended to more unconventional systems such as materials showing magnetic morphotropic phase boundaries³⁵ or martensitic phase transformations.³⁶

Acknowledgments

This effort was supported by the US Department of Energy (DOE), Office of Science Early Career Research Program (TZW), Office of Basic Energy Sciences (BES), Materials Sciences and Engineering Division, (AH, SKC) Quantum Condensed Matter Division (EJG) and the Center for Nanophase Materials Sciences (NB, CMR), which is sponsored at Oak Ridge National Laboratory by the Scientific User Facilities Division, Office of Basic Energy Sciences. The SHG work at the Iowa State University was supported by the Ames Laboratory, the US Department of Energy, Office of Science, Basic Energy Sciences, Materials Science and Engineering Division under contract DE-AC02-07CH11358. (XY, CV, JW). MSS acknowledges support from the German National Academy of Sciences Leopoldina through grant LPDS 2016-12. MSS thanks Alberto de la Torre Duran for very useful SHG discussion.

This manuscript has been authored by UT-Battelle, LLC under Contract No. DE-AC05-00OR22725 with the U.S. Department of Energy. The United States Government retains and the publisher, by accepting the article for publication, acknowledges that the United States Government retains a non-exclusive, paid-up, irrevocable, world-wide license to publish or reproduce the published form of this manuscript, or allow others to do so, for United States Government purposes. The Department of Energy will provide public access to these results of federally sponsored research in accordance with the DOE Public Access Plan (<http://energy.gov/downloads/doe-public-access-plan>).

References

- (1) Zeches, R. J.; Rossell, M. D.; Zhang, J. X.; Hatt, A. J.; He, Q.; Yang, C.-H.; Kumar, A.; Wang, C. H.; Melville, A.; Adamo, C.; et al. A Strain-Driven Morphotropic Phase Boundary in BiFeO₃. *Science* **2009**, *326* (5955), 977. <https://doi.org/10.1126/science.1177046>.
- (2) Sando, D.; Barthélemy, A.; Bibes, M. BiFeO₃ Epitaxial Thin Films and Devices: Past, Present and Future. *J. Phys. Condens. Matter* **2014**, *26* (47), 473201.
- (3) Yang, J.-C.; He, Q.; Yu, P.; Chu, Y.-H. BiFeO₃ Thin Films: A Playground for Exploring Electric-Field Control of Multifunctionalities. *Annu. Rev. Mater. Res.* **2015**, *45* (1), 249–275. <https://doi.org/10.1146/annurev-matsci-070214-020837>.
- (4) Zhang, N.; Yokota, H.; Glazer, A. M.; Ren, Z.; Keen, D. A.; Keeble, D. S.; Thomas, P. A.; Ye, Z.-G. The Missing Boundary in the Phase Diagram of PbZr_{1-x}Ti_xO₃. *Nat. Commun.* **2014**, *5*, 5231. <https://doi.org/10.1038/ncomms6231>.

- (5) Noheda, B.; Cox, D. E.; Shirane, G.; Gonzalo, J. A.; Cross, L. E.; Park, S.-E. A Monoclinic Ferroelectric Phase in the $\text{PbZr}_{1-x}\text{TixO}_3$ Solid Solution. *Appl. Phys. Lett.* **1999**, *74* (14), 2059–2061. <https://doi.org/10.1063/1.123756>.
- (6) Guo, R.; Cross, L. E.; Park, S.-E.; Noheda, B.; Cox, D. E.; Shirane, G. Origin of the High Piezoelectric Response in $\text{PbZr}_{1-x}\text{TixO}_3$. *Phys. Rev. Lett.* **2000**, *84* (23), 5423–5426.
- (7) Liu, H.; Chen, J.; Fan, L.; Ren, Y.; Pan, Z.; Lalitha, K. V.; Rödel, J.; Xing, X. Critical Role of Monoclinic Polarization Rotation in High-Performance Perovskite Piezoelectric Materials. *Phys. Rev. Lett.* **2017**, *119* (1), 017601.
- (8) Fu, H.; Cohen, R. E. Polarization Rotation Mechanism for Ultrahigh Electromechanical Response in Single-Crystal Piezoelectrics. *Nature* **2000**, *403*, 281.
- (9) Huang, Y.-C.; Liu, Y.; Lin, Y.-T.; Liu, H.-J.; He, Q.; Li, J.; Chen, Y.-C.; Chu, Y.-H. Giant Enhancement of Ferroelectric Retention in BiFeO_3 Mixed-Phase Boundary. *Adv. Mater.* **2014**, *26* (36), 6335–6340. <https://doi.org/10.1002/adma.201402442>.
- (10) Ahart, M.; Somayazulu, M.; Cohen, R. E.; Ganesh, P.; Dera, P.; Mao, H.; Hemley, R. J.; Ren, Y.; Liermann, P.; Wu, Z. Origin of Morphotropic Phase Boundaries in Ferroelectrics. *Nature* **2008**, *451*, 545.
- (11) Schlom, D. G.; Chen, L.-Q.; Eom, C.-B.; Rabe, K. M.; Streiffer, S. K.; Triscone, J.-M. Strain Tuning of Ferroelectric Thin Films. *Annu. Rev. Mater. Res.* **2007**, *37* (1), 589–626. <https://doi.org/10.1146/annurev.matsci.37.061206.113016>.
- (12) Saremi, S.; Xu, R.; Dedon, L. R.; Mundy, J. A.; Hsu, S.-L.; Chen, Z.; Damodaran, A. R.; Chapman, S. P.; Evans, J. T.; Martin, L. W. Enhanced Electrical Resistivity and Properties via Ion Bombardment of Ferroelectric Thin Films. *Adv. Mater.* **2016**, *28* (48), 10750–10756. <https://doi.org/10.1002/adma.201603968>.
- (13) Saremi, S.; Xu, R.; Allen, F. I.; Maher, J.; Agar, J. C.; Gao, R.; Hosemann, P.; Martin, L. W. Local Control of Defects and Switching Properties in Ferroelectric Thin Films. *Phys Rev Mater.* **2018**, *2* (8), 084414. <https://doi.org/10.1103/PhysRevMaterials.2.084414>.
- (14) Guo, H.; Dong, S.; Rack, P. D.; Budai, J. D.; Beekman, C.; Gai, Z.; Siemons, W.; Gonzalez, C. M.; Timilsina, R.; Wong, A. T.; et al. Strain Doping: Reversible Single-Axis Control of a Complex Oxide Lattice via Helium Implantation. *Phys. Rev. Lett.* **2015**, *114* (25), 256801.
- (15) Herklotz, A.; Rus, S. F.; Ward, T. Z. Continuously Controlled Optical Band Gap in Oxide Semiconductor Thin Films. *Nano Lett.* **2016**, *16* (3), 1782–1786. <https://doi.org/10.1021/acs.nanolett.5b04815>.
- (16) Wang, J.; Neaton, J. B.; Zheng, H.; Nagarajan, V.; Ogale, S. B.; Liu, B.; Viehland, D.; Vaithyanathan, V.; Schlom, D. G.; Waghmare, U. V.; et al. Epitaxial BiFeO_3 Multiferroic Thin Film Heterostructures. *Science* **2003**, *299* (5613), 1719. <https://doi.org/10.1126/science.1080615>.
- (17) Fu, Z.; Yin, Z. G.; Zhang, X. W.; Chen, N. F.; Zhao, Y. J.; Bai, Y. M.; Zhao, D. Y.; Zhang, H. F.; Yuan, Y. D.; Chen, Y. N.; et al. Reversible Transition between Coherently Strained BiFeO_3 and the Metastable Pseudotetragonal Phase on $(\text{LaAlO}_3)_{0.3}(\text{Sr}_2\text{AlTaO}_6)_{0.7}$ (001). *J. Appl. Phys.* **2017**, *121* (5), 054102. <https://doi.org/10.1063/1.4975342>.
- (18) Liu, H.-J.; Liang, C.-W.; Liang, W.-I.; Chen, H.-J.; Yang, J.-C.; Peng, C.-Y.; Wang, G.-F.; Chu, F.-N.; Chen, Y.-C.; Lee, H.-Y.; et al. Strain-Driven Phase Boundaries in BiFeO_3 Thin Films Studied by Atomic Force Microscopy and x-Ray Diffraction. *Phys. Rev. B* **2012**, *85* (1), 014104.
- (19) Pronin, V. P.; Dolgintsev, D. M.; Pronin, I. P.; Senkevich, S. V.; Kaptelov, E. Y.; Sergienko, A. Y. Composition Control of PZT Thin Films by Varying Technological

- Parameters of RF Magnetron Sputter Deposition. *J. Phys. Conf. Ser.* **2017**, 872 (1), 012022.
- (20) Beekman, C.; Siemons, W.; Ward, T. Z.; Chi, M.; Howe, J.; Biegalski, M. D.; Balke, N.; Maksymovych, P.; Farrar, A. K.; Romero, J. B.; et al. Phase Transitions, Phase Coexistence, and Piezoelectric Switching Behavior in Highly Strained BiFeO₃ Films. *Adv. Mater.* **2013**, 25 (39), 5561–5567. <https://doi.org/10.1002/adma.201302066>.
 - (21) You, L.; Chen, Z.; Zou, X.; Ding, H.; Chen, W.; Chen, L.; Yuan, G.; Wang, J. Characterization and Manipulation of Mixed Phase Nanodomains in Highly Strained BiFeO₃ Thin Films. *ACS Nano* **2012**, 6 (6), 5388–5394. <https://doi.org/10.1021/nn3012459>.
 - (22) Dixit, H.; Beekman, C.; Schlepütz, C. M.; Siemons, W.; Yang, Y.; Senabulya, N.; Clarke, R.; Chi, M.; Christen, H. M.; Cooper, V. R. Understanding Strain-Induced Phase Transformations in BiFeO₃ Thin Films. *Adv. Sci.* **2015**, 2 (8), 1500041-n/a. <https://doi.org/10.1002/advs.201500041>.
 - (23) Chen, Z.; Luo, Z.; Huang, C.; Qi, Y.; Yang, P.; You, L.; Hu, C.; Wu, T.; Wang, J.; Gao, C.; et al. Low-Symmetry Monoclinic Phases and Polarization Rotation Path Mediated by Epitaxial Strain in Multiferroic BiFeO₃ Thin Films. *Adv. Funct. Mater.* **2011**, 21 (1), 133–138. <https://doi.org/10.1002/adfm.201001867>.
 - (24) Christen, H. M.; Nam, J. H.; Kim, H. S.; Hatt, A. J.; Spaldin, N. A. Stress-Induced R-M_A-M_C-T Symmetry Changes in BiFeO₃ Films. *Phys Rev B* **2011**, 83 (14), 144107. <https://doi.org/10.1103/PhysRevB.83.144107>.
 - (25) Noheda, B.; Cox, D. E.; Shirane, G.; Park, S.-E.; Cross, L. E.; Zhong, Z. Polarization Rotation via a Monoclinic Phase in the Piezoelectric 92% PbZn_{1/3}Nb_{2/3}O₃ - 8% PbTiO₃. *Phys. Rev. Lett.* **2001**, 86 (17), 3891–3894.
 - (26) Lummen, T. T. A.; Gu, Y.; Wang, J.; Lei, S.; Xue, F.; Kumar, A.; Barnes, A. T.; Barnes, E.; Denev, S.; Belianinov, A.; et al. Thermotropic Phase Boundaries in Classic Ferroelectrics. *Nat. Commun.* **2014**, 5, 3172.
 - (27) Diéguez, O.; González-Vázquez, O. E.; Wojdeł, J. C.; Íñiguez, J. First-Principles Predictions of Low-Energy Phases of Multiferroic BiFeO₃. *Phys. Rev. B* **2011**, 83 (9), 094105.
 - (28) Hatt, A. J.; Spaldin, N. A.; Ederer, C. Strain-Induced Isosymmetric Phase Transition in BiFeO₃. *Phys. Rev. B* **2010**, 81 (5), 054109.
 - (29) Vanderbilt, D.; Cohen, M. H. Monoclinic and Triclinic Phases in Higher-Order Devonshire Theory. *Phys. Rev. B* **2001**, 63 (9), 094108.
 - (30) Jang, B.-K.; Lee, J. H.; Chu, K.; Sharma, P.; Kim, G.-Y.; Ko, K.-T.; Kim, K.-E.; Kim, Y.-J.; Kang, K.; Jang, H.-B.; et al. Electric-Field-Induced Spin Disorder-to-Order Transition near a Multiferroic Triple Phase Point. *Nat. Phys.* **2016**, 13, 189.
 - (31) Kan, D.; Pálová, L.; Anbusathaiah, V.; Cheng, C. J.; Fujino, S.; Nagarajan, V.; Rabe, K. M.; Takeuchi, I. Universal Behavior and Electric-Field-Induced Structural Transition in Rare-Earth-Substituted BiFeO₃. *Adv. Funct. Mater.* **2010**, 20 (7), 1108–1115. <https://doi.org/10.1002/adfm.200902017>.
 - (32) Fujino, S.; Murakami, M.; Anbusathaiah, V.; Lim, S.-H.; Nagarajan, V.; Fennie, C. J.; Wuttig, M.; Salamanca-Riba, L.; Takeuchi, I. Combinatorial Discovery of a Lead-Free Morphotropic Phase Boundary in a Thin-Film Piezoelectric Perovskite. *Appl. Phys. Lett.* **2008**, 92 (20), 202904. <https://doi.org/10.1063/1.2931706>.
 - (33) You, L.; Zheng, F.; Fang, L.; Zhou, Y.; Tan, L. Z.; Zhang, Z.; Ma, G.; Schmidt, D.; Rusydi, A.; Wang, L.; et al. Enhancing Ferroelectric Photovoltaic Effect by Polar Order Engineering. *Sci. Adv.* **2018**, 4 (7), eaat3438. <https://doi.org/10.1126/sciadv.aat3438>.
 - (34) Herklotz, A.; Gai, Z.; Sharma, Y.; Huon, A.; Rus, S. F.; Sun, L.; Shen, J.; Rack, P. D.; Ward, T. Z. Designing Magnetic Anisotropy through Strain Doping. *Adv. Sci.* **2018**, 5 (11), 1800356. <https://doi.org/10.1002/advs.201800356>.

- (35) Yang, S.; Bao, H.; Zhou, C.; Wang, Y.; Ren, X.; Matsushita, Y.; Katsuya, Y.; Tanaka, M.; Kobayashi, K.; Song, X.; et al. Large Magnetostriction from Morphotropic Phase Boundary in Ferromagnets. *Phys. Rev. Lett.* **2010**, *104* (19), 197201.
- (36) Zhang, J.; Ke, X.; Gou, G.; Seidel, J.; Xiang, B.; Yu, P.; Liang, W.-I.; Minor, A. M.; Chu, Y.; Van Tendeloo, G.; et al. A Nanoscale Shape Memory Oxide. *Nat. Commun.* **2013**, *4*, 2768.